International Commission on Illumination
Commission Internationale de l'Eclairage
Internationale Beleuchtungskommission

SPECTROSCOPIC MEASUREMENT OF FLUORESCENT PIGMENTS FOR PENETRANT TESTING

Osumi, M.

DOI 10.25039/x051.2025/kud68b

This article is also published as part of:

Proceedings of the CIE 2025 Midterm Meeting Vienna, Austria, July 4-11, 2025:
Scientific Conference (July 7-9, 2025)

DOI 10.25039/x051.2025

in

Proceedings of the CIE (International Commission on Illumination)

ISSN no. 3061-015X (print), 3061-0168 (online)

The paper has undergone double-blind peer review and its final version has been presented at the CIE 2025 Midterm Meeting, Vienna, Austria, July 4–11, 2025.

CIE Central Bureau
Babenbergerstrasse 9/9A
A-1010 Vienna, Austria
Tel.: +43 1 714 31 87
e-mail: ciecb@cie.co.at — www.cie.co.at

 DOI: 10.25039/x051.2025/kud68b

SPECTROSCOPIC MEASUREMENT OF FLUORESCENT PIGMENTS FOR PENETRANT TESTING

Osumi, M.[1]

[1] Office Color Science Co.,LTD., Kumamoto, JAPAN

masayuki-osumi@nifty.com

Abstract

The purpose of this study was to rationalize the Fluorescent Penetrant Test, which is used for crack inspection of building structures, equipment, and various parts, and to establish a method for measuring fluorescent images using spectral imaging. As the fluorescent agent, five types of water-soluble fluorescent colour paints with different excitation-emission wavelength ranges were used. The fluorescence properties of the fluorescent agent were performed using a spectrofluorometer comprising two spectrometers. For spectral imaging, an LED lamp emitting UV light was used for illumination, and a light receiving device composed of a liquid crystal tunable filter and a monochrome CCD sensor was used. As a result of the measurement, we were able to obtain an excitation-emission matrix and a spectroscopic image, and based on this, it became possible to study how to obtain high contrast in inspection.

Keywords: Penetrant test, Fluorescent, Measurement, Spectral imaging

1 Introduction

The penetrant test method (ISO3059:2012) is used for flaw detection and inspection of building structures and equipment involving welding. Among them, the fluorescent penetrant test is a method of visual observation by irradiating the test surface with ultraviolet rays in a dark place using a penetrant containing a fluorescent substance, and it is possible to detect even very small scratches with high detection sensitivity. However, the intensity of ultraviolet light emitted by the ultraviolet light source used for observation, the amount of visible light at the observation site, and the fluorescence and spectral characteristics of the fluorophore may greatly affect the visibility of the flaw detection. In this study, we prepared a sample of a building exterior tile in which fluorescent pigments were infiltrated into artificially generated cracks, and performed spectral imaging measurements using UV light for illumination with the aim of establishing an optical model for fluorescent penetrant testing and improving the efficiency of the test. In addition, the spectral characteristics of the fluorescent penetrant used were measured by an excitation-fluorescence matrix using a spectrofluorometer based on the two-spectrometer method.

2 Experimental

2.1 Sample Preparation

2.1.1 For fluorescent material measuring

The fluorescent solution used was an acrylic water-based Glow Paint made by Neon nights in the U.S., in which five colours, White, Green, Pink, Orange, and Yellow, were diluted in water. In order to measure fluorescence properties of these five colours, BYK Chart brightened 2A, which is a hiding power test strip (ASTM D344 compliant) for paints that is contain no optical brighteners, was applied using a painting brush, and then dried naturally at room temperature to be used as a sample for spectrofluorometer measurement as figure 1.

2.2.2 For Crack Sample measuring by spectral imaging

The ceramic tiles of a building material with a side of 30 cm square and a thickness of 5 mm were selected as the target material for the flaw detection test. The back of the tile was

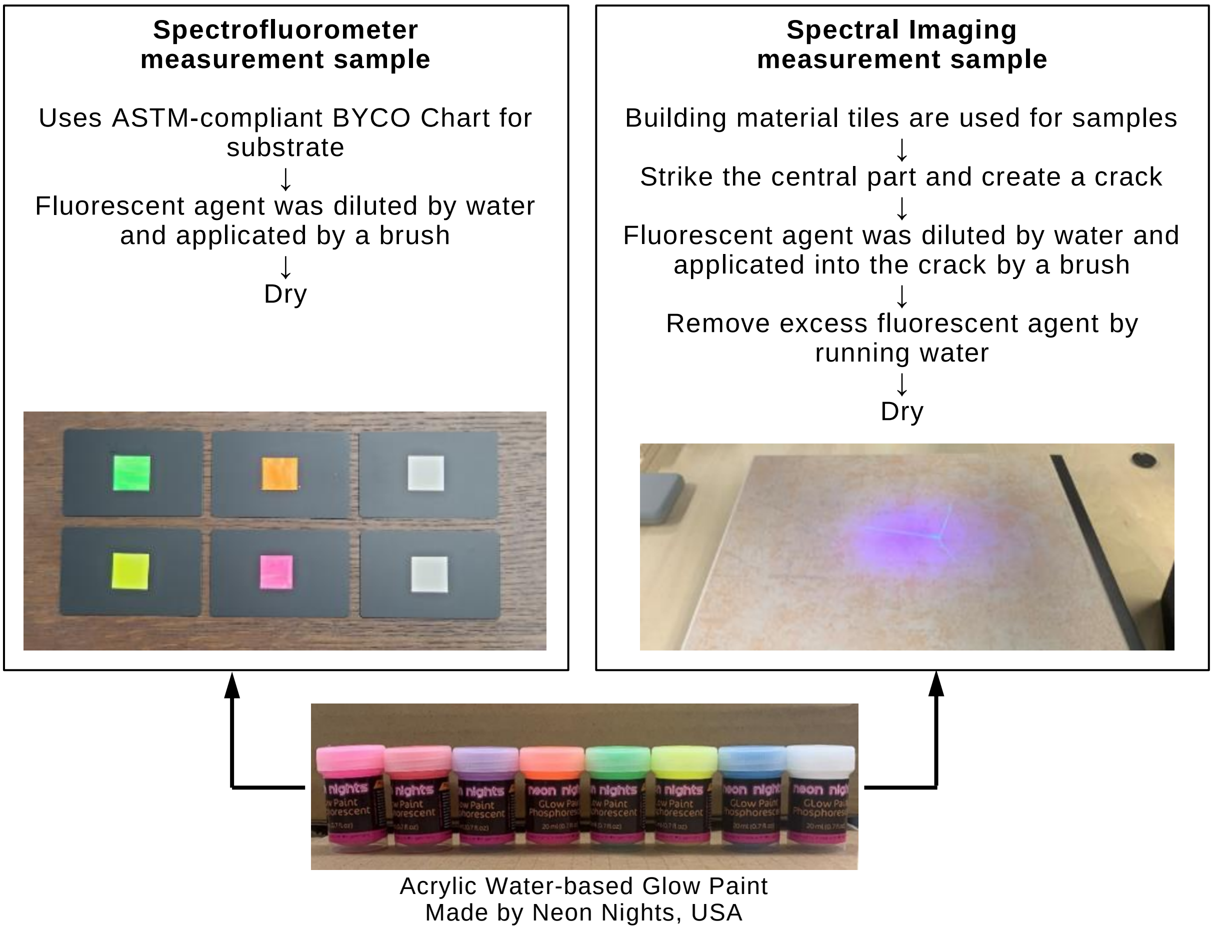

Figure 1 – Sample preparation

reinforced with adhesive tape to prevent shattering, spacers with a thickness of about a few millimetres were applied to the four corners, and cracks were artificially generated by striking the centre of the tile with a mallet. Fluorescent penetrant was applied and permeated into the cracks, and the excess infiltrated on the surface was washed off with water, and then dried naturally at room temperature (see figure 1). These were measured by irradiating it with LED UV light as excitation light. As a reference, figure 2 shows a situation in which only fluorescent lamps, both fluorescent lamps and UV lights, and only UV light were irradiated to the created crack tile sample. The visibility of the crack was dramatically improved when UV light was used alone.

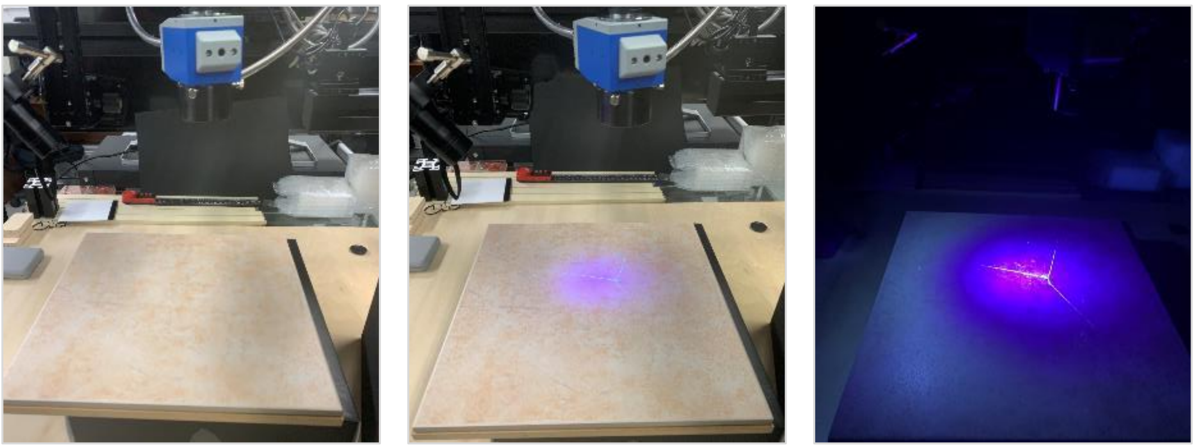

Fluorescent light only | Fluorescent light + UV light | UV light only

Figure 2 – The crack sample for the measurement under several illuminations

 DOI: 10.25039/x051.2025/kud68b

2.2 Measurement of fluorescent materials by spectrofluorometer

The excitation-emission matrix, which is a characteristic unique to fluorescence, was measured using the F-7100 spectrofluorometer manufactured by Hitachi Hitec, Japan. This spectrophotometer purpose is scientific analysis for the measurement of fluorescence phenomena, and performs monochromatic light illumination with a spectrometer using a xenon lamp as a light source on the irradiation side, and a spectro-photoreceptor with a reflective diffraction grating and a photomultiplier tube on the light receiving side. As a result, it is possible to measure the excitation-emission matrix (EEM) using the two-spectrometer method, and it is possible to realize separate measurement of scattered light and fluorescence (see figure 2). In this study, since the purpose of this study was to observe and quantify the fluorescence phenomenon caused by ultraviolet irradiation, monochromatic light irradiation was performed every 5 nm in the range of 300 nm to 700 nm on the excitation side, and every 5 nm in the range of 300 nm to 700 nm on the receiving side. The slit width was 2.5 nm on both the irradiation side and the light receiving side, and the calibration data was obtained using a Spectralon manufactured by Labsphere of the United States, which has reflectance data traceable to NIST. The measurement sample plates were mounted at an angle of 30° with respect to the light receiving direction, and were installed so that specular reflection was not received.

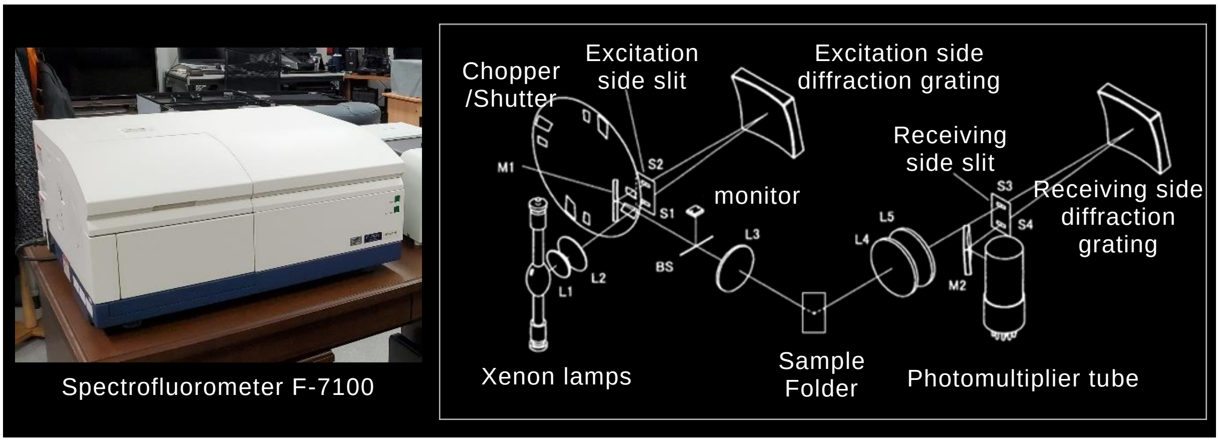

Figure 2 – Spectrofluorometer

2.3 Measurement of crack samples by spectral imaging

The spectral imaging system consisted of a photo receiving system installed in the vertical direction of the sample surface, a liquid crystal tunable filter (VariSpec manufactured by CRi in the U.S.) as a spectroscopic measure, and a monochrome CCD sensor with a 16-bit output equipped with Peltier cooling and an anti-blooming mechanism. The sensor had 772×580 pixels and the captured resolution was 627 dpi. The UV light was irradiated at an angle of about 45 degrees from the vertical direction of the sample surface. The wavelength ranged from 420 nm to 700 nm, and a total of 29 wavelengths were measured every 10 nm. The bandwidth of the liquid crystal tunable filter was about 10 nm. In addition, an integrating sphere with a diameter of 20 cm was used for calibration of the system before measurement.

At the time of calibration, the white standard plate is targeted, but the sensitivity of each pixel and the effect of peripheral dimming of the optical system are corrected. In addition, this system is devised to automatically optimize the exposure time for each measurement wavelength during calibration. As a result, the difference in wavelength sensitivity of the CCD and the transmittance of each wavelength of the liquid crystal tunable filter can be corrected, and good measurement results can be obtained in all pixels and all measurement wavelength ranges. In addition, since this device does not have an operating mechanism, it is possible to suppress the occurrence of streaks due to vibration and other errors during scanning.

The configuration of the measurement system is shown in figure 3, and the spectral distribution of the UV light used for measurement is shown in figure 4.

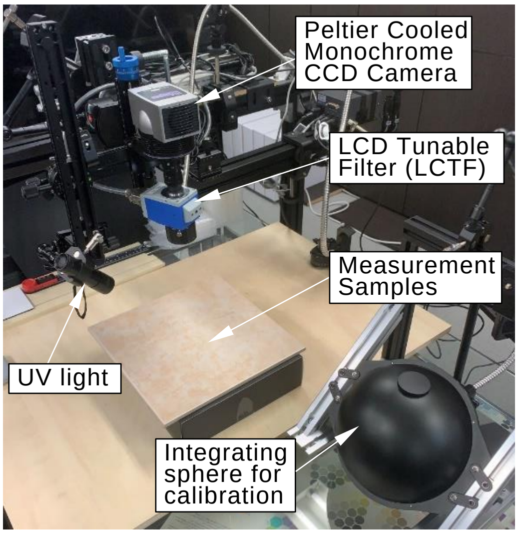

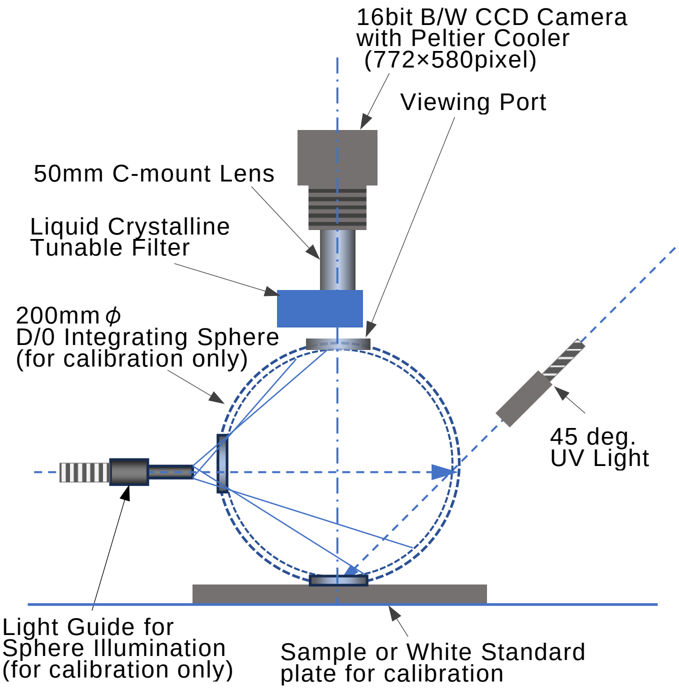

Figure 3 – Spectral imaging measurement system

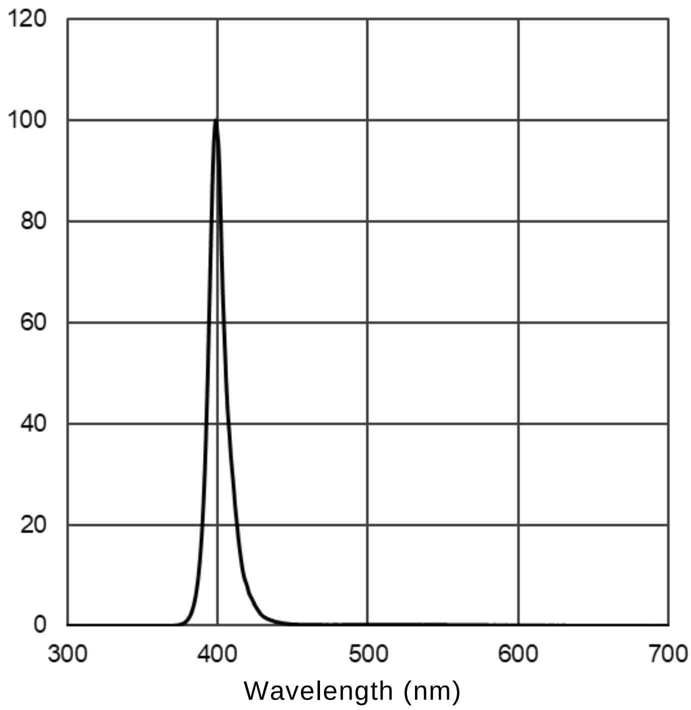

UV light

Figure 4 – The relative spectral distribution of UV light source for the spectral Imaging measurement

3 Result

3.1 The excitation-emission matrix measurement result by spectrofluorometer

Figure 3 shows the results of the excitation-emission matrix (EEM) measurement of seven measurement samples, including the back side of the BYK Chart without Spectralon and fluorescent penetrant. In the individual graphs, the vertical direction is the excitation wavelength, the lower end is 300 nm and the upper end is 700 nm, and the horizontal direction is the light receiving wavelength on the fluorescence side, which is 300 nm at the left end and 700 nm at the right end. Therefore, the diagonal region from the lower left to the upper right, where the excitation wavelength and the received wavelength coincide, captures the reflected light in the non-fluorescent region. In the case of fluorescence phenomena, according to Stokes' law, the received wavelength λ_{EM} appears in the region longer than the excitation wavelength λ_{EX}. Therefore, in the figure, the part that appears on the lower side of the diagonal region becomes the fluorescent component. In the BYK Chart, almost no fluorescence phenomena were observed, and in the standard reflector Spectralon used for calibration, there was no fluorescence phenomenon. On the other hand, fluorescence phenomena were observed in all fluorescent penetrants, and fluorescent components were remarkably detected in Yellow and Orange. And the fluorescent component of White fluorescent penetrant is not observed so strongly, and the reflective component in the non-fluorescent region is strongly observed in the visible light region. It is presumed that the fluorescent agent used of White is only make a brightening effect.

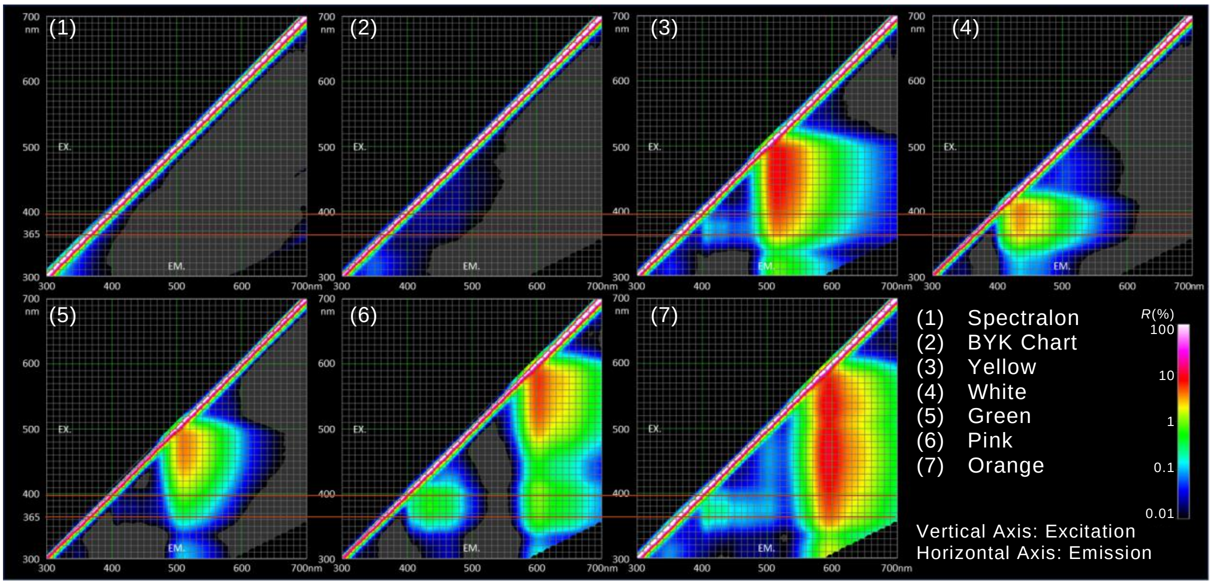

Figure 6 – Excitation – emission matrix of 7 measurement sample

3.2 Measurement result by spectral imaging

Cracks that are almost invisible under fluorescent lamps are dramatically increased when fluorescent penetrant is applied and illuminated with UV light (figure 2). The penetrant test shown in ISO3059:2012 takes advantage of this characteristic. The measurement results using UV light irradiation are shown in figure 7 to 10. The right side of figure 7, and the figure 8 shows the composite images of each wavelength after spectral imaging measurements. The crack is permeated with a fluorescent agent, and it can be seen that fluorescence is emitted by excitation light.

The left side of figure 7 shows the spectroscopic information of the area indicated by the blue line corresponding to the length of 5 mm that crosses the crack in the measurement result shown on the right side of figure 7 in a 3D graph. In the 3D graph, the planar direction is the axis of wavelength and position, and the lines indicating the crack and position capture the fluorescence radiation at exactly the intersecting position. At 420~430 nm, the non-fluorescent reflected light of the tiles due to UV light irradiation is captured. For the four types of fluorescence, Green, Orange, Yellow, and Pink, the peak wavelength of fluorescence is longer than 500 nm, and separation of fluorescence and non-fluorescence regions can be expected, but for White, as fluorescence brightening, ultraviolet rays are absorbed and light is emitted from 430 nm to 470 nm, so separation cannot be expected. This is consistent with the measurement results of the excitation-emission matrix by the spectrofluorometer described above.

Figure 10 shows the individual measurement results of the five measurement samples, and the measurement images for each wavelength of each fluorescent penetrants are shown in 20 nm increments from 430 nm to 610 nm. In the 430 nm image, the reflection in the non-fluorescent region of the tile itself is remarkable.

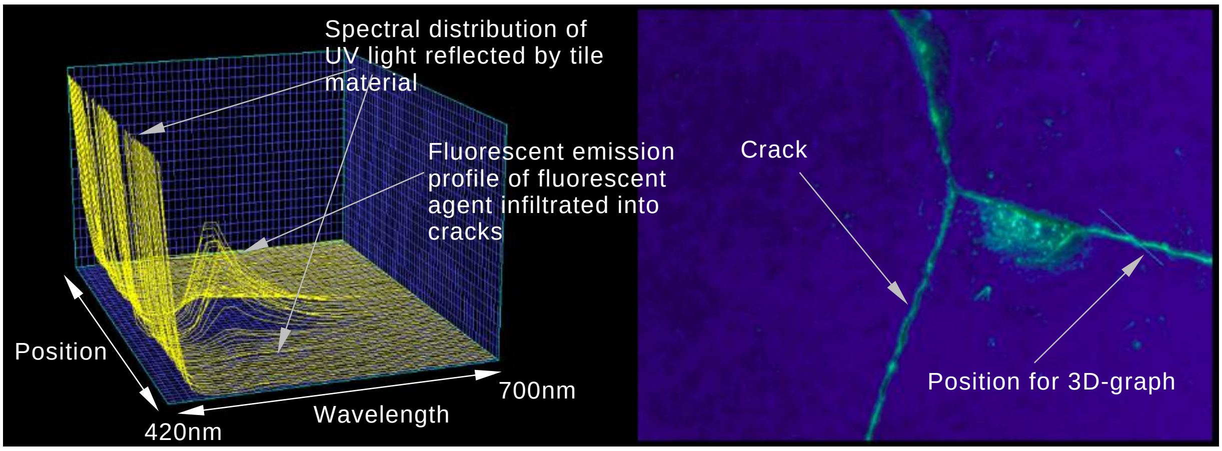

Figure 7 – Spectral Imaging measurement result (Green tile example)

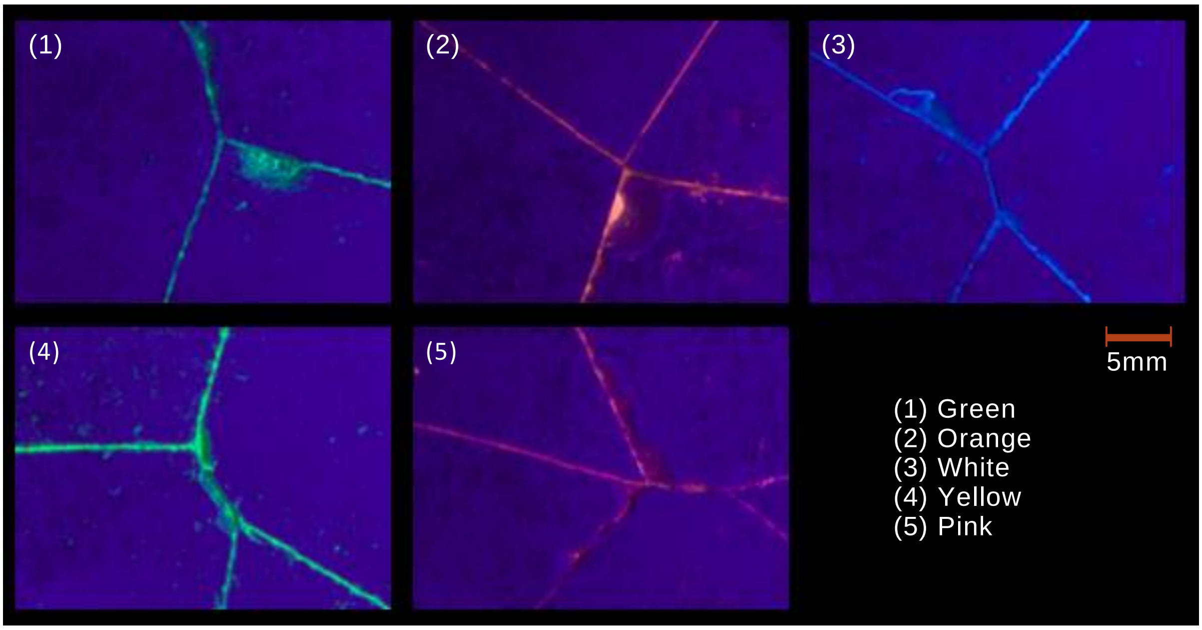

Figure 8 – Measurement result by spectral imaging of 5 crack samples (Visual image)

 DOI: 10.25039/x051.2025/kud68b

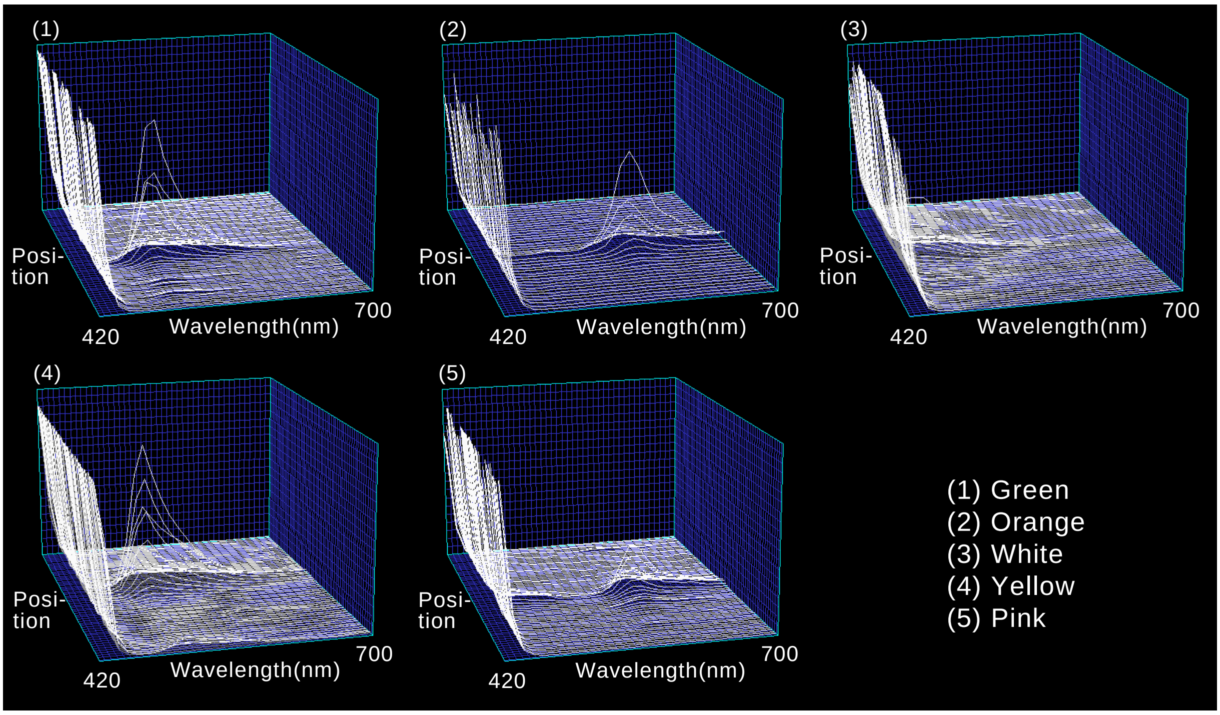

Figure 9 – Measurement result by spectral imaging of 5 crack samples (3D-graph)

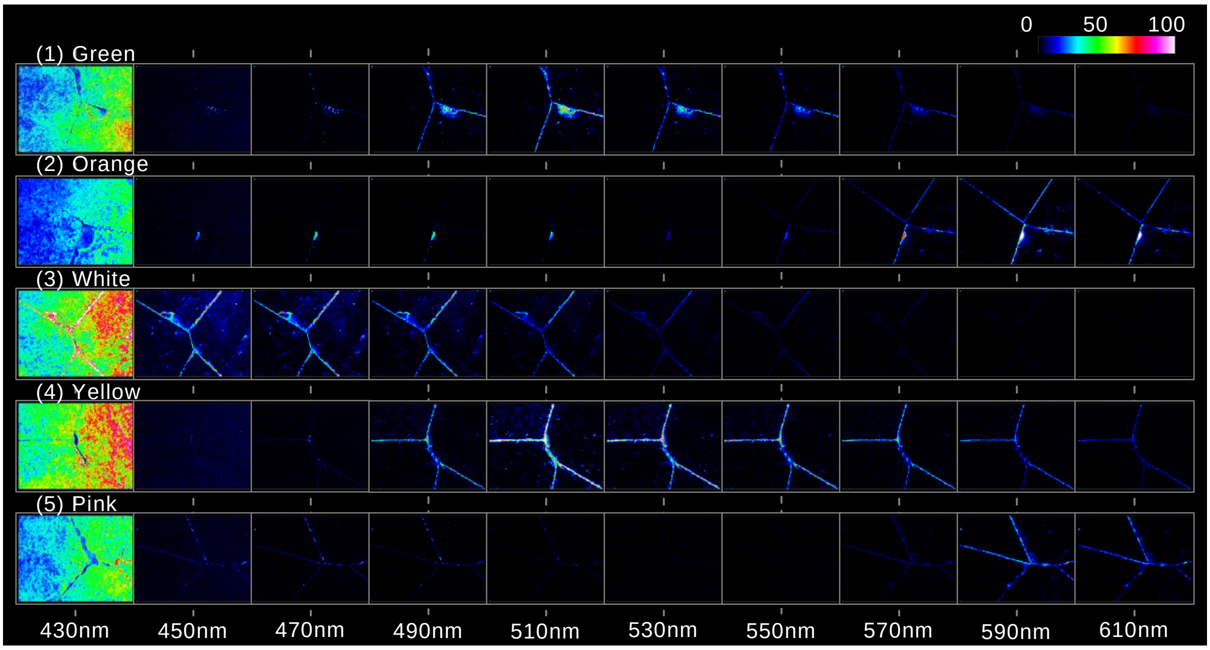

Figure 10 – Measurement result by spectral imaging of 5 crack samples (Each 20nm wavelength)

3.3 Consideration

In the fluorescent penetrant test, the penetration of the fluorescent substance into the crack is observed in a dark place by fluorescence emission excited by UV light, and it is essential to obtain excellent visibility and facilitate flaw detection. Therefore, the irradiance and spectral distribution of UV light, the fluorescence emission efficiency (quantum yield) of the fluorophore based on the irradiation spectral distribution, the spectral reflectance and optical anisotropy of the flaw detection target, and the contrast between the ambient light and the fluorescence emission at the visual viewing position affect the visibility.

When buildings such as bridge piers and buildings are subject to inspection, it is not always possible to perform visual inspections in an absolutely dark environment, and the effects of moonlit nights and urban light are also considered. Along with this, the visual characteristics also change. Depending on the degree of ambient light, the spectral luminous efficiency will vary between $V(\lambda)$ and $V'(\lambda)$. In addition, under a certain amount of ambient light, the reflection characteristics and texture of the object to be inspected are also considered to have an effect. Since fluorescence emission is Lambertian, EEM is not affected by geometric conditions, but if the surface of the test object is glossy or has optical anisotropy, the direction of irradiation of stray light and the geometric conditions observed can also be considered as factors of influence. In short, the spectral reflection characteristics of the observation target, the spectral characteristics of ambient light, the reflection and fluorescence characteristics of the EEM of the fluorescent penetrant, the spectral response of the observer side, and the optical geometric conditions of these optical geometric conditions require simulation and optimization of contrast. These concepts and elements are shown in Figure 11.

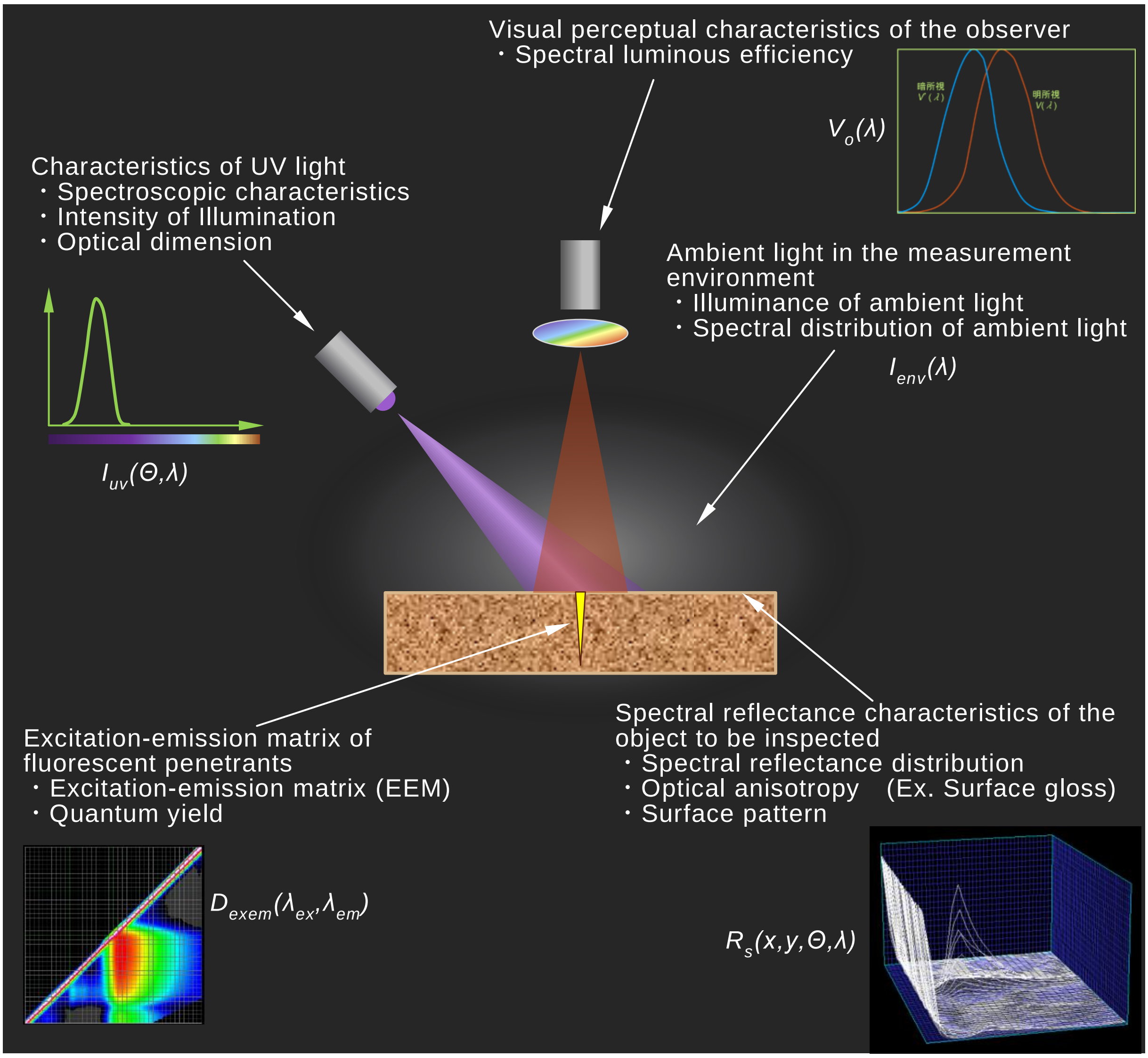

Figure 11 – Optimal concepts and elements of fluorescent penetrant test

In ISO3059:2012, the maximum intensity of the irradiated light observed is 365 nm ± 5 nm and the half-width is 30 nm. However, the fluorescent agent measured in this study does not necessarily have the maximum excitation in this vicinity. In addition, considering the effect of ultraviolet light on the human body, it is desirable to irradiate light on the long wavelength side as much as possible. ISO3059:2012 specifies the test method for fluorescent penetrants, but the fluorescence intensity described in the Appendix is measured using a fluorometer with excitation light at 365 nm, and the sensitivity measurement is limited to the method of visual perception under the conditions of ISO3059:2012.

In this study, the method for a series of measurements of each element was explored. Figure 12 shows the contrast when irradiated with UV light with a peak wavelength of 395 nm and observed at a spectral luminous efficiency *V*(λ). In this case, Yellow had the best visibility. It is desirable to search for an optimal method that considers the overall relationship between UV light, fluorescent agent, measurement target, and spectral characteristics of ambient light.

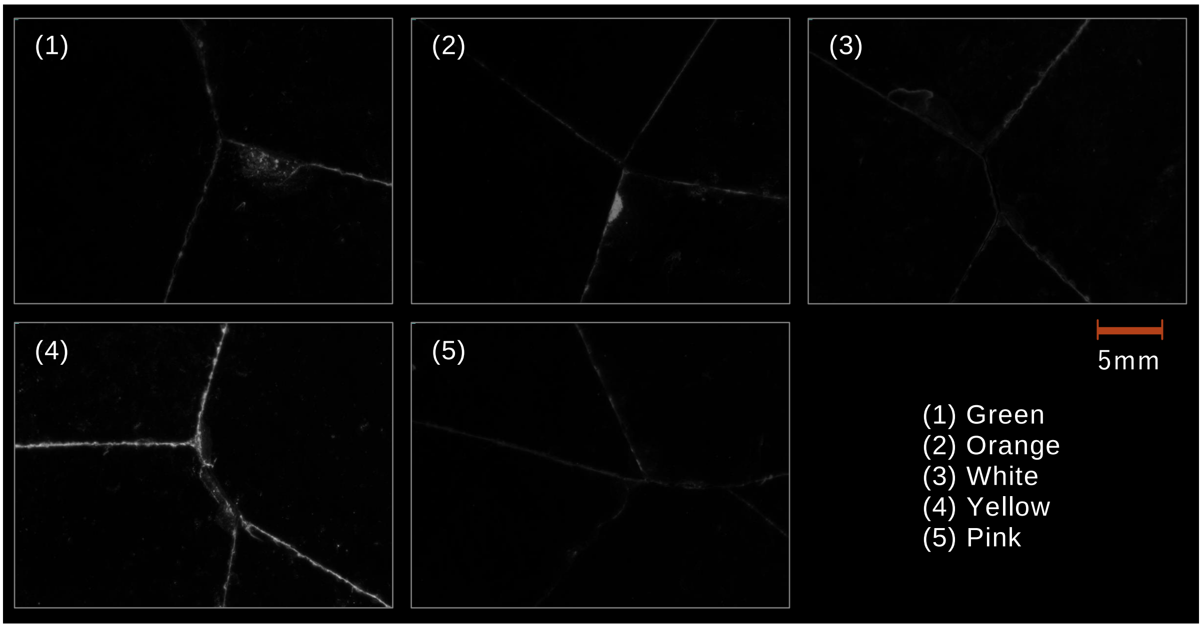

Figure 12 – The contrast image of 5 crack samples under 395 nm UV light using *V*(λ)

References

ISO 2010. ISO 3059:2012. Non-destructive testing — Penetrant testing and magnetic particle testing — Viewing conditions. ISO

TANG, Y., NIU, A., WEE, W.G., and HAN, C.Y. 1995. Automated inspection system for detecting metal surface cracks from fluorescent penetrant images: SPIE 2423, Machine Vision Applications in Industrial Inspection III

YUN, Y., MIN, Z., ZUO, J., HAN, B. and LI, L. 2022. Crack identification of automobile steering knuckle fluorescent penetrant inspection based on deep convolutional generative adversarial networks data enhancement. Physical Acoustics and Ultrasonics. Volume 10 - 2022.

MIGOUN, N.P., DELENKOVSKII, N.V. 2009. Improvement of penetrant testing methods. Journal of Engineering Physics and Thermophysics. Volume 82, pages 734-742.